Supplementary Information

Increased carbon capture by a silicate-treated forested watershed affected by acid deposition

Lyla L. Taylor[1*], Charles T. Driscoll[2], Peter M. Groffman[3], Greg H. Rau[4], Joel D. Blum[5] and David J. Beerling[1]

[1]Leverhulme Centre for Climate Change Mitigation, Department of Animal and Plant Sciences, University of Sheffield, Sheffield S10 2TN, UK

[2]Department of Civil and Environmental Engineering, 151 Link Hall, Syracuse University, Syracuse, NY 13244, USA

[3]City University of New York, Advanced Science Research Center at the Graduate Center, New York, NY 10031 and Cary Institute of Ecosystem Studies, Millbook, NY 12545 USA

[4]Institute of Marine Sciences, University of California, Santa Cruz, CA 95064 USA

[5]Department of Earth and Environmental Sciences, University of Michigan, Ann Arbor, MI 48109, USA

Correspondence to: Lyla L. Taylor (L.L.Taylor@sheffield.ac.uk)

1 Geochemistry

1.1 Carbonic acid equilibria

In an open system where gaseous CO_2 is not limited, such as water in contact with the air, Henry's Law means that carbonic acid is linearly proportional to the partial pressure of CO_2 gas ($pCO_2(g)$):

$$[H_2CO_3^*] = K_H \times pCO_2(g) \quad \text{(S1)}$$

where hydrated CO_2 ($CO_2(aq)$) and carbonic acid (H_2CO_3) are combined as $H_2CO_3^*$. Speciation of carbonate and bicarbonate ions is given by equilibria depending on $[H_2CO_3^*]$ and on $[H^+]$, where $pH = -\log_{10}[H^+]$:

$$[HCO_3^-] = [H_2CO_3^*] \times [H^+] \times K_1 \quad \text{(S2)}$$

$$[CO_3^{2-}] = [HCO_3^-] \times [H^+] \times K_2 = [H_2CO_3^*] \times [H^+]^2 \times K_1 K_2 \quad \text{(S3)}$$

Similar equilibrium expressions apply to organic acids.

1.2 Alkalinity, major ions and acids

Relationships between SO_4^{2-}, NO_3^- and organic and carbonic acids can be illustrated via expressions for alkalinity. Following Stumm and Morgan (Stumm and Morgan 1996), a simple expression for freshwater alkalinity is given by:

$$Alk = [HCO_3^-] + 2[CO_3^{2-}] + [OH^-] - [H^+] \quad \text{(S4a)}$$

Equation S4a excludes non-carbonate alkalinity found in New Hampshire rivers (Hunt, Salisbury, and Vandemark 2011), but can be modified to include species related to the organic acid H_3A from Equation 1d:

$$Alk = [HCO_3^-] + 2[CO_3^{2-}] + [OH^-] - [H^+] + [H_2A^-] + 2[HA^{2-}] + 3[A^{3-}] \quad \text{(S4b)}$$

A general alkalinity expression including non-carbonate alkalinity (Stumm and Morgan 1996) is:

$$Alk = [HCO_3^-] + 2[CO_3^{2-}] + [OH^-] - [H^+] + [NH_3] + [HS^-] + 2[S^{2-}] + [H_3SiO_4^-] + 2[H_2SiO_4^{2-}] + [B(OH)_4^-]$$
$$+ [A^-] + [HPO_4^{2-}] + 2[PO_4^{3-}] - 2[H_2PO_4^{2-}] \quad \text{(S4c)}$$

where A is a collective term for organic acids . Boric acid species $[H_3BO_3]$ and $[B(OH)_4^-]$ are included in seawater.

In practice, CO_3^{2-} is usually neglected in CO_2 consumption calculations (Raymond 2017) because it is several orders of magnitude smaller than HCO_3^- within the typical pH range of most natural waters [4.5-9]. In this pH range, an alternative definition of alkalinity, based on major ions (Stumm and Morgan 1996), arises from the requirement for electrical neutrality of the solution:

$$Alk = 2([Ca^{2+}] + [Mg^{2+}] - [SO_4^{2-}]) + [K^+] + [Na^+] + [NH_4^+] - [NO_3^-] - [Cl^-] - [F^-] \quad \text{(S5)}$$

The anions and cations in eqn. S5 are associated with fully dissociated acids and bases in the pH range of natural waters, as described above. Consequently, they strongly control streamwater chemistry and pH ($-\log_{10}[H^+]$) because S4a or S4b must equal S5. Speciation of organic and carbonic acids depends on pH, so these weak acids react to conditions created by the major ions. Eqns. 4 and 5 suggest that changes to any major ion in Eqn. S5 will result in concomitant adjustments in the ions

of 4. In turn, Eqns 4a and 4b imply that, given the major ions, ignoring the organic acid could increase the calculated bicarbonate concentrations.

1.2 Carbonate mineral weathering

It has been common to treat forests with carbonate minerals such as $CaCO_3$ (calcite or aragonite) or $CaMg(CO_3)_2$ (dolomite) to mitigate the effects of anthropogenic acidification. Here we present $CaCO_3$ weathering equations analogous to our wollastonite equations (1–4, main manuscript):

$$CaCO_3 + H_2O + CO_2 \leftrightarrows Ca^{2+} + 2HCO_3^- \quad \textbf{(S6)}$$

$CaCO_3$ weathering by carbonic acid results in two bicarbonate ions, one from the $CaCO_3$ and one from the atmosphere. It will effectively raise the pH of the solution, but compared to wollastonite weathering (1, main manuscript), it draws down half the CO_2 from the atmosphere. When a new $CaCO_3$ molecule is precipitated by an organism or by evaporation, the second bicarbonate ion will be released as CO_2 to maintain charge balance of the solution.

$$CaCO_3 + H_2SO_4 \rightarrow Ca^{2+} + H_2O + CO_2 + SO_4^{2-} \quad \textbf{(S7)}$$
$$CaCO_3 + 2HNO_3 \rightarrow Ca^{2+} + H_2O + CO_2 + 2NO_3^- \quad \textbf{(S8)}$$
$$CaCO_3 + 2H_3A \rightarrow Ca^{2+} + H_2O + CO_2 + 2H_2A^- \quad \textbf{(S9)}$$

Following $CaCO_3$ weathering by other acids, the resulting acid-derived anions will prevent the formation of bicarbonate and result in release of CO_2 derived entirely from the weathered $CaCO_3$. Bicarbonate formation requires neutralization of these acid-derived anions.

Dolomite weathering obeys a similar set of equations. Ion production is effectively doubled compared to $CaCO_3$ weathering, as each dolomite molecule is equivalent to one $CaCO_3$ plus one $MgCO_3$ molecule:

$$CaMg(CO_3)_2 + 2H_2O + 2CO_2 \leftrightarrows Ca^{2+} + Mg^{2+} + 4HCO_3^- \quad \textbf{(S10)}$$
$$CaMg(CO_3)_2 + 2H_2SO_4 \rightarrow Ca^{2+} + Mg^{2+} + 2H_2O + 2CO_2 + 2SO_4^{2-} \quad \textbf{(S11)}$$
$$CaMg(CO_3)_2 + 4HNO_3 \rightarrow Ca^{2+} + Mg^{2+} + 2H_2O + 2CO_2 + 4NO_3^- \quad \textbf{(S12)}$$
$$CaMg(CO_3)_2 + 4H_3A \rightarrow Ca^{2+} + Mg^{2+} + 2H_2O + 2CO_2 + 4H_2A^- \quad \textbf{(S13)}$$

Equations **S7** and **S10** show that carbonate mineral weathering by carbonic acid (eqns **S6** and **S10**) draws down half the atmospheric CO_2 of silicate weathering per cations released. Because silicate minerals do not contain carbon, they cannot release CO_2 when weathered. Silicate minerals are therefore of greater interest than carbonate minerals in the context of CDR.

1.3 Use of strontium isotopes as calcium tracers

Our use of Eqn. 10 (Methods) to determine the fraction X_{Ca} originating from wollastonite (**Fig. S1a**) follows the widely-held assumption that strontium (Sr) is an isotopic tracer of calcium provenance (Nezat, Blum, and Driscoll 2010; Peters et al. 2004). Being divalent cations in the same group in the periodic table, Sr and Ca have similar chemical behaviour and only slightly differing atomic radii. Strontium can therefore replace calcium in a variety of minerals, in particular plagioclase and apatite. Incorporation of Sr within mineral lattices in place of Ca is favoured by eight-fold coordination with oxygen (Capo, Stewart, and Chadwick 1998).

Rubidium (Rb) substitutes for K in minerals, but because ^{87}Rb decays to ^{87}Sr, and because ^{86}Sr and ^{87}Sr are both stable isotopes, the ratio $^{87}Sr/^{86}Sr$ is distinctive for rocks of similar age and Rb/Sr ratio. The $^{87}Sr/^{86}Sr$ ratio can also trace the provenance of Sr in soil, pore waters, pedogenic carbonates and other secondary minerals because these pools have the same isotopic composition as the source material(Capo, Stewart, and Chadwick 1998). Isotopic fractionation is insignificant during chemical weathering, physical erosion and atmospheric transport (Bain and Bacon 1994) as well as biological processes (Capo, Stewart, and Chadwick 1998) including nutrient uptake.

Changes in Ca/Sr ratios due to any of the above processes are minor (Blum et al. 2002), but some processes do lead to partitioning between Ca and Sr which may need to be accounted for (Pett-Ridge, Derry, and Barrows 2009). For example, Sr is more strongly retained in soils than Ca (Capo, Stewart, and Chadwick 1998), and partitioning also occurs during biogeochemical cycling processes such as nutrient uptake and within-plant transport (Pett-Ridge, Derry, and Barrows 2009). In a study of apatite weathering at Hubbard Brook, the two molar ratios $^{87}Sr/^{86}Sr$ and Ca/Sr were found to be distinctive for atmospheric inputs, bedrock silicates and apatite (**Fig. S1b**).

Comparison with these three end-members suggested that streamwaters, pore waters and particularly the soil exchange pool held little apatite-Ca (Blum et al. 2002). $^{87}Sr/^{86}Sr$ was found to be similar in the leaves of different species of trees, ferns, soil exchangers, soil and stream waters, and soil apatite, while Ca/Sr was distinctive (Blum et al. 2002). Together, these two ratios suggested that apatite was an important source of calcium for the dominant forest trees other than Ca-sensitive *Acer saccharum* in the treated watershed prior to the wollastonite treatment (Blum et al. 2002).

The wollastonite used in our experiment was formed by contact metamorphism between silica and limestone (Virta 2000). Its $^{87}Sr/^{86}Sr$ ratio is therefore typical of limestone (Capo, Stewart, and Chadwick 1998) and consequently easily distinguished from other Ca sources (Blum et al. 2002) at the HBEF. Like the apatite found in these soils (Blum et al. 2002), it has a high Ca/Sr ratio, whereas pre-treatment streamwater Ca/Sr was considerably lower (Peters et al. 2004). Peters et al (Peters et al. 2004) showed that the applied wollastonite was also isotopically distinct from pretreatment streamwater and that streamwater ratios during the first year after treatment could be explained by mixing between these two end-members (Fig. S4b). Ca/Sr during the infiltration period 3+ years post-treatment appears to show a slight tendency towards apatite (**Fig. S1b,c**) but this is expected as ~35% of streamwater Ca was derived from apatite prior to treatment (Blum et al. 2002).

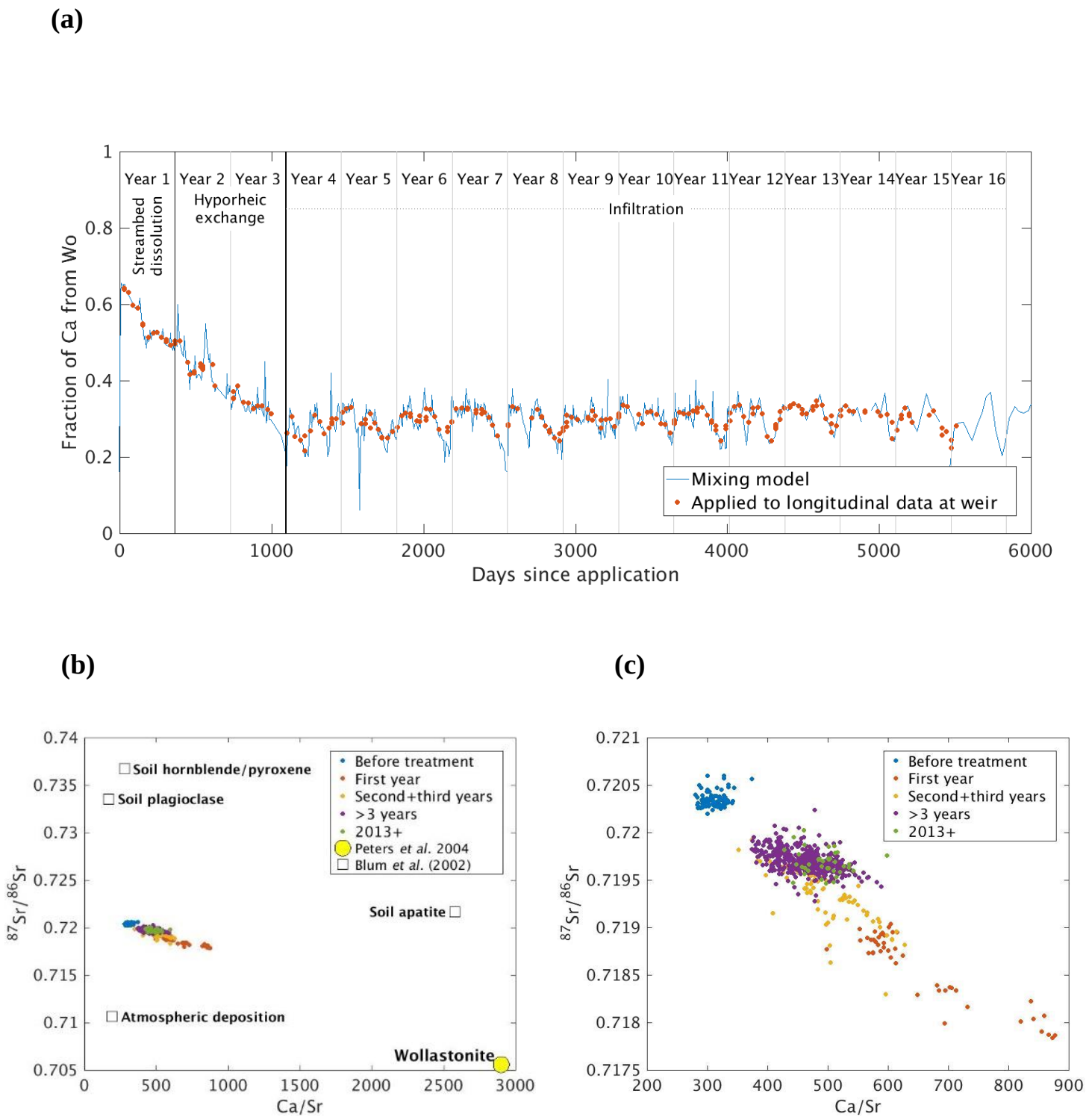

Figure S1. Strontium as a tracer. (a) Contribution of wollastonite Ca to streamwater Ca^{2+} in the treated watershed, using the mixing model of Peters et al (Peters et al. 2004) and showing the conceptual model of Nezat et al (Nezat, Blum, and Driscoll 2010). This mixing model assumes that mixing is linear between two endmembers. According to the conceptual model, wollastonite-derived Ca did not appear in streamwater until three years had elapsed. Subsequent work has supported this conceptual model (Shao et al. 2016). (b) Ca/Sr and Sr isotopic ratios change following treatment, suggesting a change in provenance toward wollastonite (Peters et al. 2004) rather than toward other calcium sources (Blum et al. 2002). (b) Blum et al (Blum et al. 2002) found that ~35% of the Ca in pretreatment streamwater originated from apatite weathering; this signal is still apparent during the infiltration period (>3 years post-treatment).

2 CO_2 consumption at Hubbard Brook

When calculated using bicarbonate and carbonate ions, CO_2 consumption ($CO_{2,HCO3}$) depends strongly on the pH of the streamwater, which was similar for our two watersheds prior to treatment (**Fig. S2a**). After treatment, pH rose sharply in the treated watershed but soon approached values only slightly higher than the reference watershed.

CO_2 consumption is directly proportional to flow rates, which are slightly lower in the treated watershed (**Fig. S2b**), particularly in late summer (**Fig. S2c**). Consideration of the total rolling annual streamflow, where each point is the sum of the flow over the preceding 365 days, shows that flow was higher in the reference watershed prior to treatment and for several years following treatment (**Fig. S2d**).

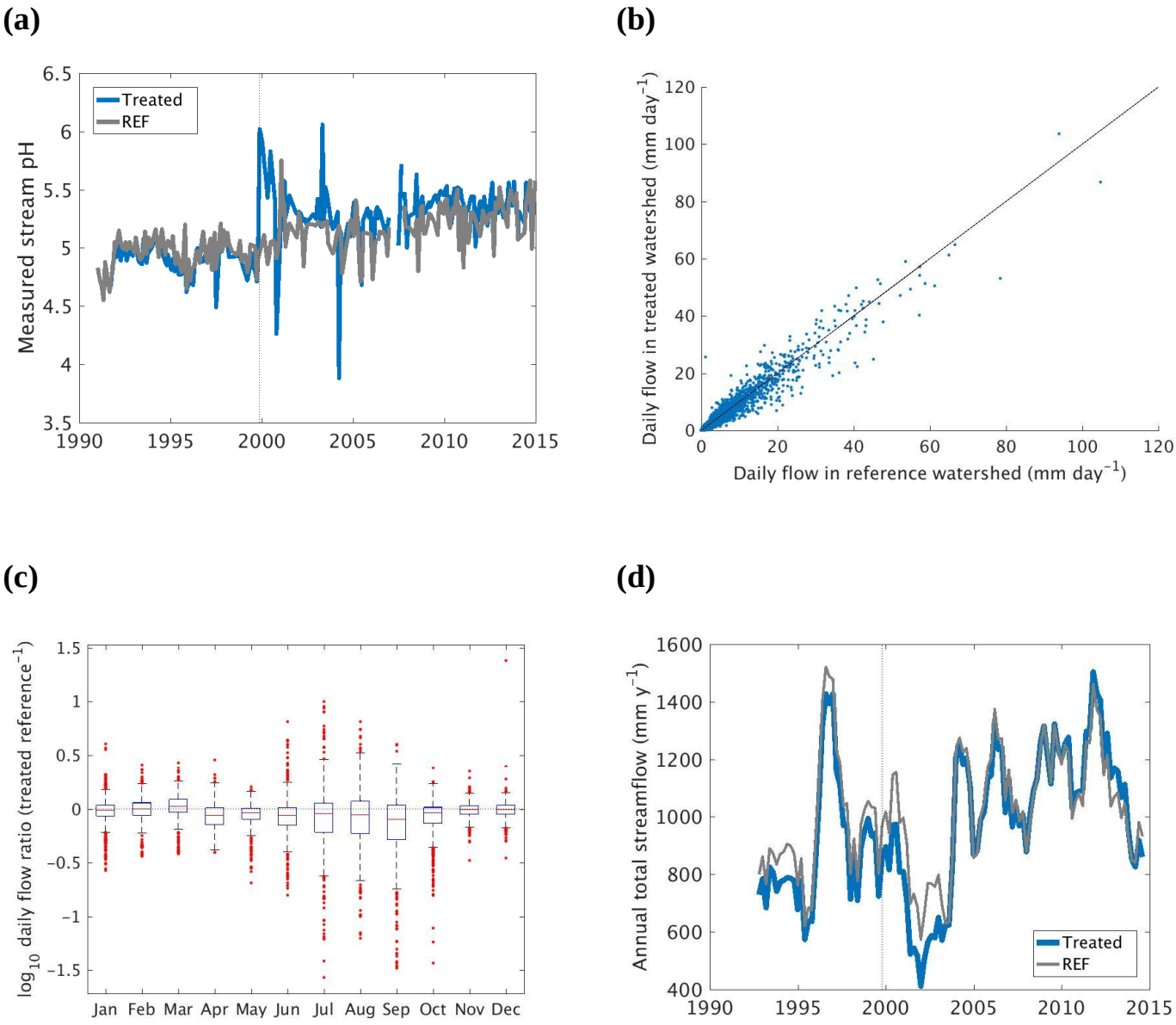

Figure S2. Comparison of the treated and reference watersheds since 1991. (a) Streamwater pH, (b) total daily flow, (c) ratio of treated/reference daily flow on a monthly basis displayed as boxplots (center line median, box limits upper and lower quartiles, whisker length 1.5×interquartile range, including all outliers (•) and (d) rolling annual streamflow, where each point is the sum of the preceding 365 days. Note that the reference watershed dataset (Driscoll 2016b) extends into the 1980s whereas the treated watershed dataset (Driscoll 2016a) does not.

2.1 Contribution of rainwater to CO_2 consumption fluxes

Calculation of rainwater contributions is described in the Methods. **Fig. S3** shows the rainwater contribution to bicarbonate, while **Fig. S4** shows rainwater contributions to Na^+, Ca^{2+}, SO_4^{2-}, and NO_3^-. Note that the nitrate spikes discussed in the main text (2012–2015) are not contributed by rainwater.

Many authors correct cation-based CO_2 consumption for SO_4^{2-} originating from weathering ($CO_{2,ions}$, see Methods in main text), but at HBEF SO_4^{2-} is largely derived from rainwater. In principle, all the SO_4^{2-} at the HBEF is from acid deposition via rainwater, but some had been sorbed to soil oxides and was desorbed following treatment. The simple rainwater correction shown in **Fig. S4** may not account for SO_4^{2-} desorbed from soil oxides (**Fig. S4**), but this legacy SO_4^{2-} still originates from atmospheric deposition. Because total SO_4^{2-} will reduce CO_2 consumption ($CO_{2,HCO3}$ or $CO_{2,ions}$) along with marine alkalinity and therefore storage of bicarbonate in the water column, we do not apply any rainwater correction to SO_4^{2-} when calculating $CO_{2,ions}$.

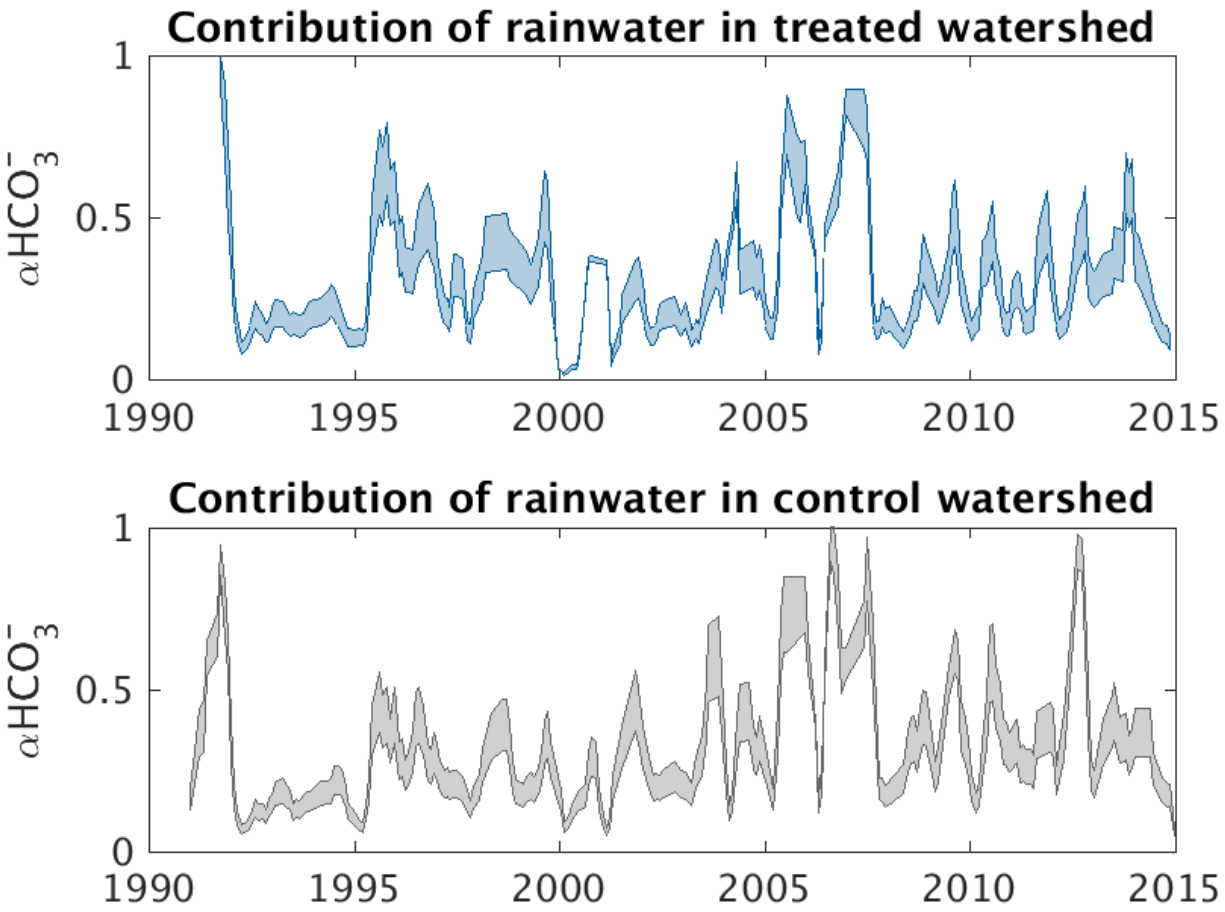

Figure S3. Contribution of rainwater in treated (top) and reference (bottom) watersheds. In each panel, the bottom of the envelope corresponds to the higher atmospheric CO_2 simulations. A three-point smoothing has been applied to these curves.

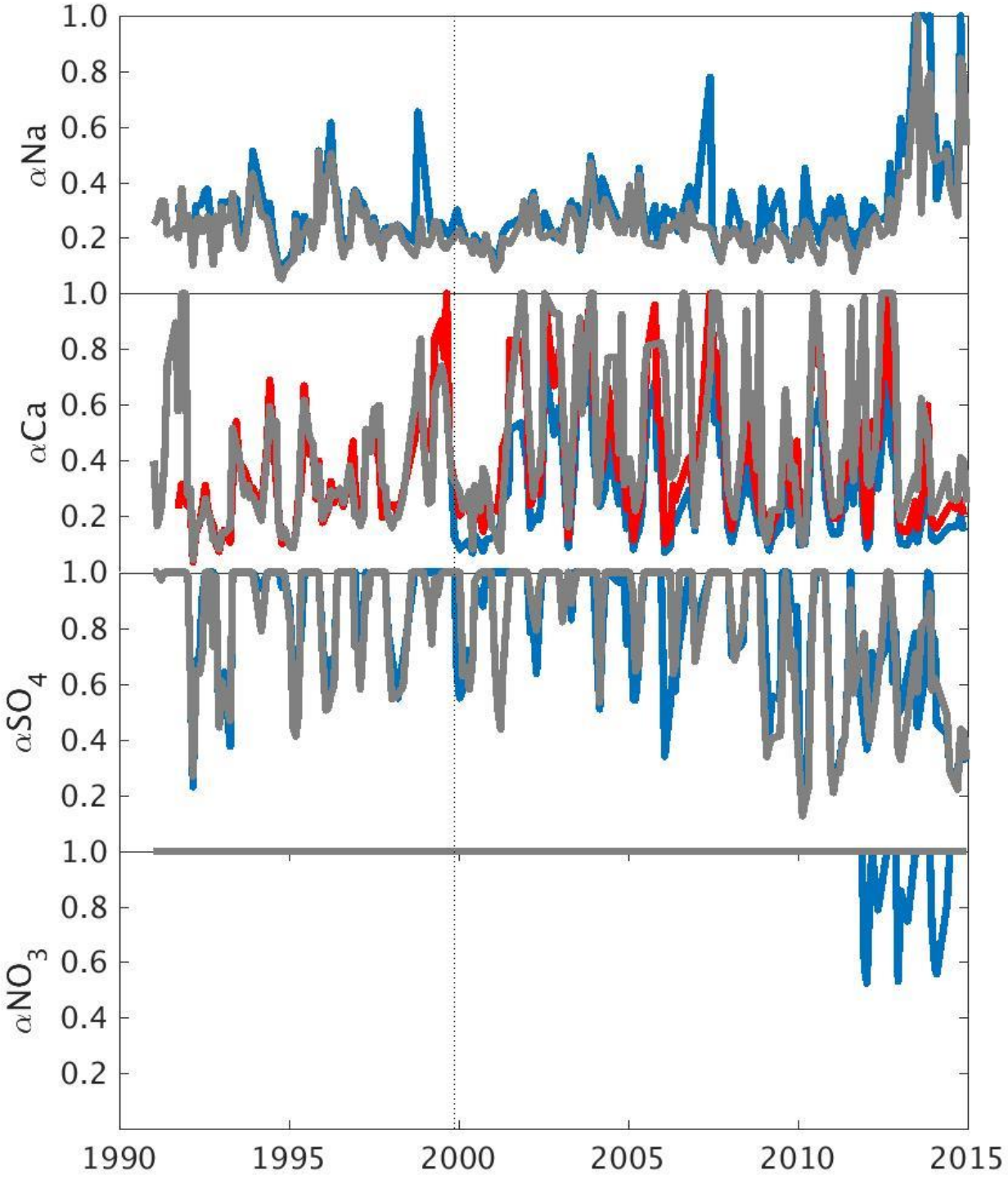

Figure S4. Fractional contribution of rainwater to Na^+, Ca^{2+}, SO_4^{2-}, and NO_3^- for our baseline case in the treated watershed. The bottom and top axes for each panel represent 0 (no rainwater contribution) and 1 (all from rainwater) respectively. The time of treatment is indicated with a vertical dotted line.

2.2 Comparison with literature

Our annual CO_2 consumption estimates are within the ranges of most previous estimates for Hubbard Brook watersheds (**Table S1**). We estimate that 2% of the applied Wo-Ca was exported during the first six years following treatment, and 4% was exported by the end of year 11. These are within the range of prior published studies (Shao et al. 2016; Cho et al. 2012). Our mean treatment-related CO_2 consumption rates for the period 2003–2012 were Wo-$CO_{2,HCO3}$=0.004 and Wo-$CO_{2,Ca}$=0.02 mol C m^{-2} y^{-1}. The latter corresponds to 43.9 kg Wo-Ca yr^{-1}, four-times higher than predicted by Nezat et al (Nezat, Blum, and Driscoll 2010), but similar to results presented by Shao et al (Shao et al. 2016) (49.4 kg Wo-Ca yr^{-1}). Our estimated Wo-Ca export rate suggests that increased CO_2 consumption following treatment could last for ~140 yrs, i.e., the time taken to deplete the 14 metric tons of calcium applied to the treated watershed.

Table S1. Estimates of annual CO_2 consumption at the treated and reference catchments Hubbard Brook. Where calculated from wollastonite-derived calcium (Wo-Ca) export, perfect efficiency is assumed following 1.

CO_2 consumption			**Catchment**	**Method**	**Period**	**Source**
t CO_2 ha^{-1}	**g C m^{-2} y^{-1}**	**mol C m^{-2} y^{-1}**				
0.0044	0.12	0.01	REF (6)	H^+ accounting	pretreatment	(Fahey et al. 2005)
0.0009	0.024	0.002	REF (6)	Bicarbonate, 5	pretreatment–2002	This study
0.0013	0.036	0.003	REF (6)	Bicarbonate, 5	mean, 2003–2014	This study
0.0004	0.012	0.001	Treated (1)	Bicarbonate, 5	pretreatment	This study
0.0110	0.30	0.025	Treated (1)	Wo-Ca export	mean, 1999–2010	(Schlesinger and Amundson 2018) their SI
0.0048	0.133	0.011	Treated (1)	Wo-Ca export	mean, 1999–2010	(Shao et al. 2016) their Table 1
0.0048	0.132	0.011	Treated (1)	Wo-Ca export	mean 2003–2010	(Shao et al. 2016) their Table 1
0.0022	0.056	0.005	Treated (1)	Wo-Ca export	mean 2005–2008	(Nezat, Blum, and Driscoll 2010)
0.0084	0.228	0.019	Treated (1)	Wo-Ca, 9	mean 2003–2014	This study
0.0018	0.048	0.004	Treated (1)	Bicarbonate, 7	mean 2003–2014	This study
per unit watershed area						
0.0167	0.459	0.038	Treated (1)	Wo-Ca export	year 1	(Hartmann and Kempe 2008)
0.0260	0.703	0.059	Treated (1)	Wo-Ca export	year 1	(Peters et al. 2004)
0.0216	0.586	0.049	Treated (1)	Wo-Ca export	year 1	(Shao et al. 2016) their Table 1
0.0229	0.625	0.052	Treated (1)	Wo-Ca, 9	year 1	This study
0.0048	0.132	0.011	Treated (1)	Bicarbonate, 7	year 1	This study
per unit streambed area						
1.1003	30	2.5	Treated (1)	Wo-Ca export	year 1	(Hartmann and Kempe 2008)
1.6843	45.96	3.827	Treated (1)	Wo-Ca export	year 1	(Peters et al. 2004)
1.4044	38.33	3.191	Treated (1)	Wo-Ca export	year 1	(Shao et al. 2016) their Table 1
1.4981	40.88	3.404	Treated (1)	Wo-Ca, 9	year 1	This study
0.3164	8.634	0.719	Treated (1)	Bicarbonate, 7	year 1	This study

2.3 Sensitivity to other acids

At Hubbard Brook, CO_2 consumption as computed with bicarbonate ($CO_{2,HCO3}$) was reduced due to the presence of environmental acids other than carbonic acid, as discussed in the main text. **Fig. S5** shows the solute concentrations, solute fluxes and CO_2 consumption curves for the sulphuric acid (**Fig. S5a,b,c**), nitric acid (**Fig. S5d,e,f**) and organic acid (**Fig. S5g,h,i**) scenarios described in **Section 3.2** of the main text.

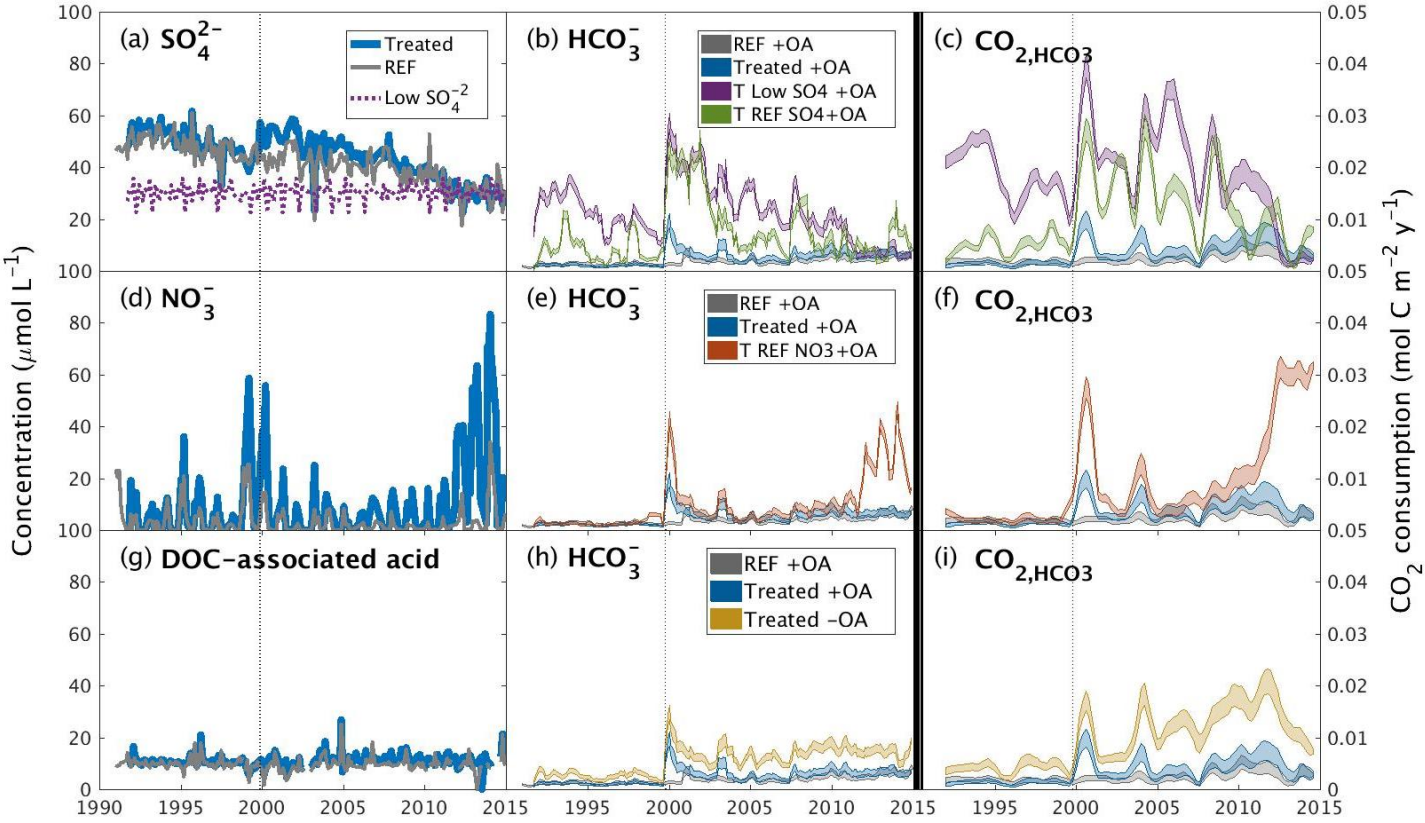

Figure S5. Sensitivity of watershed inorganic CO_2 capture at Hubbard Brook to environmental change. Modelled watershed steamwater bicarbonate and corresponding patterns of total CO_2 consumption ($CO_{2,HCO3}$ by Eq. 5) and treatment-associated CO_2 consumption (Wo-$CO_{2,HCO3}$ by Eq. 7) following (a–c) removal of acid deposition effects ("Low SO4" scenario) or (d–f) removal of transient nitrate spiking ("REF NO3" scenario), and (g–i) sensitivity to the presence or absence of organic acids (OA+ and OA-, respectively). Bicarbonate concentrations (b,e,h) for all scenarios are shown to the same scale. All CO_2 consumption curves (c,f,i) are shown to the same scale and were calculated with flow-normalised concentrations and corrected for sparsity of samples (Methods).

2.4 Sensitivity to treatment size

As discussed in the main text **Section 3.3**, **Fig. S6** shows the increases in calcium and bicarbonate concentrations (**Fig. S6a**), rolling annual CO_2 consumption (**Fig. S6b**), and cumulative CO_2 consumption (**Fig. S6c**) given a ten-fold larger wollastonite treatment.

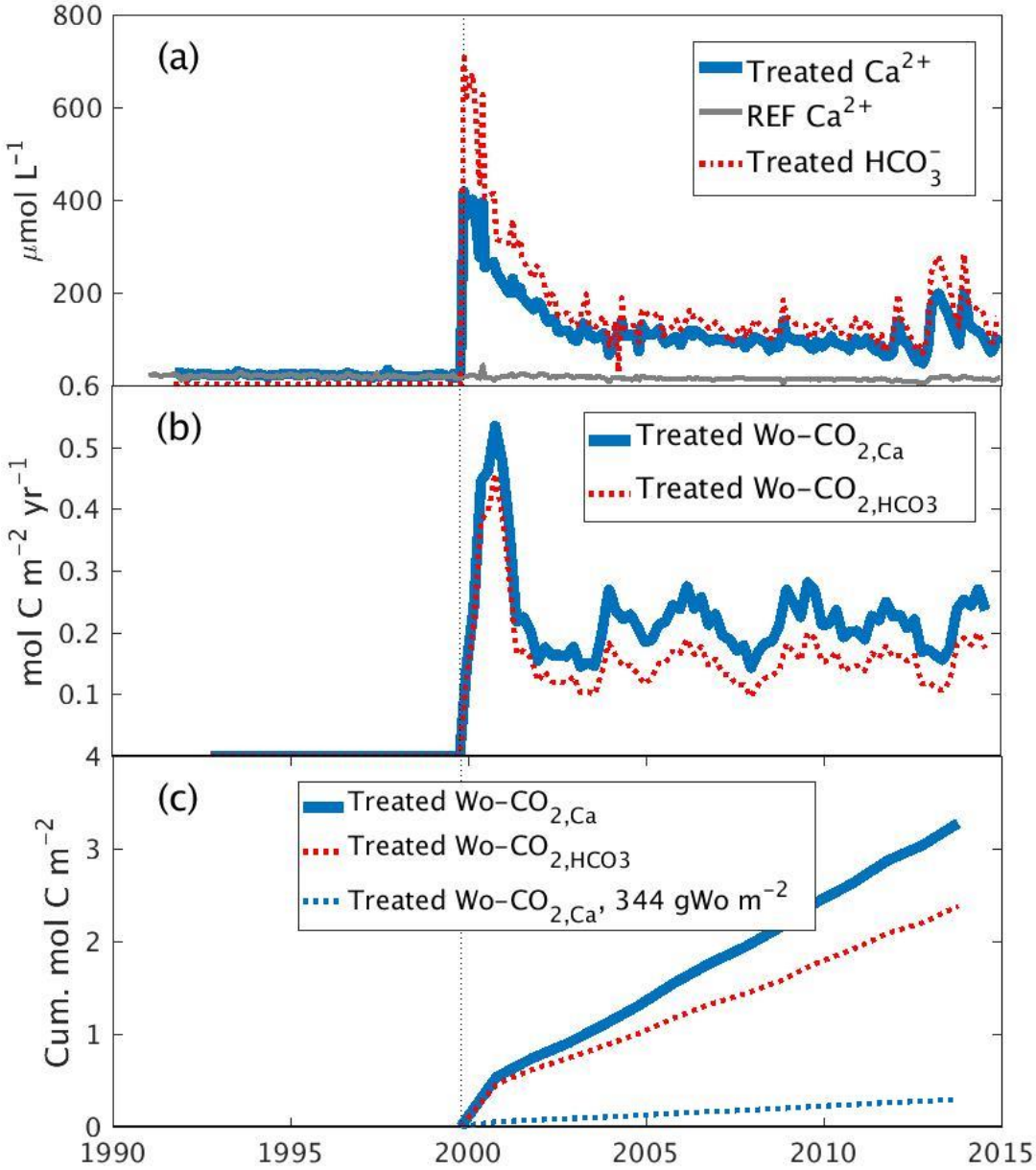

Figure S6: Simulated inorganic CO_2 capture for a 10-fold higher wollastonite treatment in the Hubbard Brook Experimental Forest. (a) Calcium and bicarbonate concentrations, along with observed reference calcium. Calcium is charge-balanced by up to two moles of bicarbonate. (b) CO_2 consumption due to this higher treatment (Wo-$CO_{2,Ca}$ and Wo-$CO_{2,HCO3}$) and (c) Cumulative CO_2 consumption for both this higher treatment and the actual treatment (Wo-$CO_{2,Ca}$). We have assumed that a 10-fold higher treatment produces 10-fold higher calcium concentrations with no change in sulphate, nitrate or DOC. Simulated HCO_3^- concentration and Wo-$CO_{2,HCO3}$ account for the presence of organic acids (+OA) given observed DOC. All CO_2 consumption curves (b,c) were flow-normalised and corrected for sparsity of samples (Methods).

3 Downstream effects

3.1 Degassing in the HBEF streams, rivers and near-shore environments

If CO_2 consumption is determined by bicarbonate ($CO_{2,HCO3}$, 5), it will be subject to substantial temporal and spatial variability due in part to riverine CO_2 outgassing linked to geomorphological heterogeneities, seasonality, and changes in connectivity with subsurface water flows (Duvert et al. 2018). Hubbard Brook, for example, is part of the larger Merrimack Watershed that experiences large seasonal CO_2 degassing before and after entering the Merrimack estuary (Salisbury et al. 2008).

Progressive degassing begins in the steep headwaters of the HBEF, and continues far downstream of the weirs where our samples were collected. Near the Merrimack river mouth, waters are typically oversaturated with respect to atmospheric CO_2 gas in November (~1200 µatm) and undersaturated in July (Salisbury et al. 2008), suggesting seasonal degassing along the length of the river. In the Merrimack estuary, the fresh river water forms a buoyant plume extending into the Gulf of Maine. As a result of wind-driven mixing with the underlying salt water (Chen, MacDonald, and Hetland 2009), the surface water approaches equilibrium with atmospheric CO_2 by degassing in November or acting as a CO_2 sink in July (Salisbury et al. 2008). Dissolved carbon concentration (DIC) is therefore extremely sensitive to location and timing. In equilibrium with atmospheric CO_2, peak DIC and CO_2 consumption in the treated watershed decrease by over 70% (not shown).

Degassing in estuaries is inversely related to DIC and buffering capacity (Bauer et al. 2013) and may represent wetland microbial respiration rather than riverine carbon (Cai 2011). For some large, alkaline rivers with high-pCO_2 estuaries, degassing represents only a small fraction of the DIC transported to the ocean (Cai 2011). Globally, estuaries export 10% more carbon seaward than to the atmosphere, but continental shelves are undersaturated because transport across the shelves only takes a few months (Bauer et al. 2013). Unfortunately, the complex interplay between aquatic heterotrophs and productivity, and labile dissolved organic carbon (DOC) and nutrient fluxes on carbon cycling in estuaries is not well understood (Bauer et al. 2013; Salisbury et al. 2008).

The amount and duration of DIC storage at sea may depend on poorly understood processes of air-sea gas exchange and remineralisation rates of sinking organic matter (Williamson et al. 2012) as well as regional limitations on nutrient supply to the ocean surface and thus to marine photosynthesis (Williamson et al. 2012; Marinov et al. 2008). ERW with basalt may increase phosporus and iron fluxes to the oceans, but at present there is no protocol for representing the contribution of such nutrient fluxes for carbon accounting.

These processes indicate that streamwater DIC will not reflect carbon sequestration in the ocean water column, and indeed CO_2 consumption and longer-term storage are more closely related to streamwater alkalinity (Renforth and Henderson 2017). We have not explicitly addressed degassing in our study, although we have considered effects of weathering by acids other than carbonic acid (Eqns. 2–4 main text), and downstream greenhouse gas emissions associated with nitric and organic acids.

3.2 Dissolved organic carbon

The chemistry and isotopic composition of marine DOC indicates it is largely of marine origin (Bianchi 2011), implying net removal of terrestrial DOC before it reaches the high seas. At low latitudes, terrestrial DOC may be oxidised in coastal waters over continental shelves, contributing to CO_2 degassing fluxes (Cai 2011). Our pessimistic assumption is that all excess exported DOC (associated with the treatment) is oxidised or respired downstream, leading to CO_2 emissions and therefore to a carbon penalty. The relevance of organic acids associated with marine DOC for marine DIC storage is unclear, as is the

interplay between ERW and terrestrial DOC contributions to degassing. However, policy-makers should be aware that DOC-related organic acids can affect total alkalinity measurements in low-pH, organic-rich streamwaters, if carbon-based CO_2 consumption ($CO_{2,HCO3}$, 5) is employed for verification.

265

3.3 Nitrate

Nitrate export in streamwater is unlikely to affect marine storage because of its low concentrations in seawater far from the coast. At least 80% of inorganic nitrogen is denitrified in coastal waters (Seitzinger and Giblin 1996; Bauer et al. 2013) under low-oxygen conditions caused by eutrophication, but denitrification is associated with greenhouse gas (N_2O) emissions
270 (Canfield, Glazer, and Falkowski 2010) which could counteract CO_2 sequestration achieved with ERW. This greenhouse gas penalty can be quantified by converting streamwater nitrate to N_2O emissions in rivers and estuaries, and converting N_2O to equivalent carbon dioxide emissions (CO_{2e}) as described in Methods. In our study, the absolute magnitude of this penalty (**Fig. 3c** and **Table 2**, main manuscript) exceeded bicarbonate-derived CO_2 consumption associated with the wollastonite treatment (Wo-$CO_{2,HCO3}$). In view of these results and the nitrate-treatment interactions observed at Hubbard Brook(Rosi-
275 Marshall et al. 2016), near-shore N_2O emissions could be enhanced by other rock dust treatments on land. Although $CO_{2,HCO3}$ (CO_2 consumption calculated with bicarbonate) is sensitive to nitrate, sulphate and organic acids, it cannot fully account for the complex C and N dynamics of nearshore environments.

4 Forest effects

4.1 Soil respiration, other soil greenhouse gas emissions and elevation

280 Greenhouse gas measurements were made in four vegetation zones which are characterised by different tree species composition and different responses to the wollastonite treatment. We carried out statistical analyses of our measured data (**Fig. S7, S8** and **S9**) as described in the main text. Reduced cumulative soil respiration in the high-elevation hardwood zone in the treated watershed (**Fig. 2**, main text) may be related to lower fine root biomass observed in 2013 compared to 1998 (Fahey et al. 2016) rather than microbial decomposition. Although the treatment resulted in significant increases in hardwood
285 leaf litter decay relative to a nearby control site (Lovett, Arthur, and Crowley 2016) and significant decreases in organic matter and carbon in the Oa horizon relative to pre-treatment (Johnson et al. 2014), it is not clear that these effects were elevation dependent or how the Oa horizon compares with the reference watershed. However, soils were more depleted in Ca at higher elevation than at lower elevations, and the Ca-sensitivity of *Acer saccharum* Marsh. increases with increasing elevation (Minocha et al. 2010).

290 Our monthly measurements showed no significant effects for soil N_2O emissions (**Fig. S8**). Similar to an earlier study comparing the HBEF valley to the highest HBEF elevations (Groffman et al. 2009b), we found that the lower-elevation hardwood soils were stronger sinks for CH_4 than higher elevation hardwood soils in the treated watershed (**Fig. S9, S10**). In the reference watershed, however, mid- to high-elevation hardwoods have been smaller sinks than low-elevation hardwoods since 2002 (**Fig. S10**).

295 ### 4.2 Trees as a sink for calcium

We considered the possibility that the extra wood production identified by Battles et al (Battles et al. 2014) could have explained part of the discrepancy in the calcium budget identified by previous authors (Shao et al. 2016). Given ~661 μgCa g^{-1}wood (Arthur, Siccama, and Yanai 1999), this effect amounts to 8.8 mmol Ca m^{-2}, well below the missing 1822.5 out of 2570 mmol Wo-Ca m^{-2} applied (Shao et al. 2016). The Wo-Ca budget remains unclosed.

300

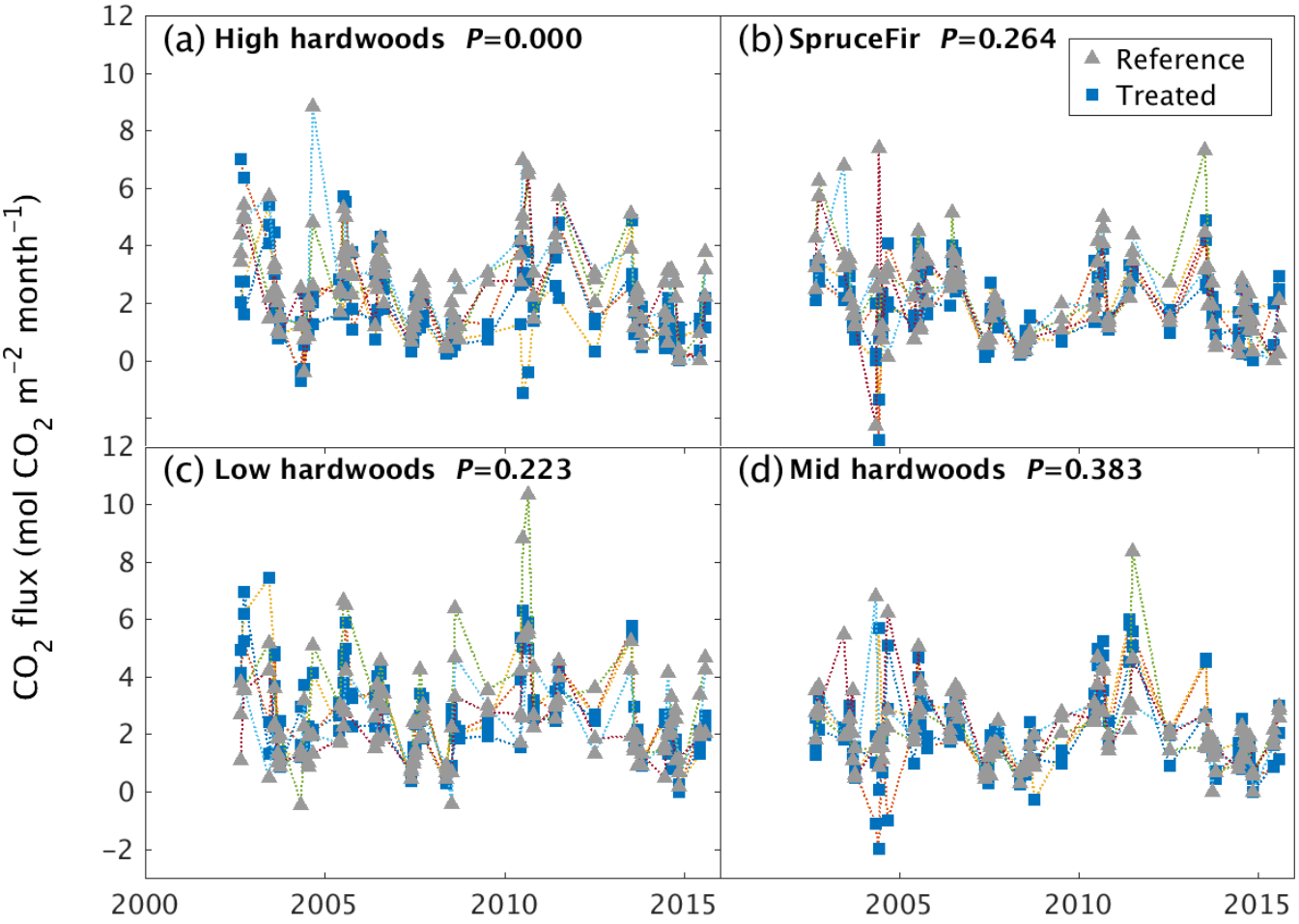

Figure S7. Soil respiration for four vegetation types: (a) SpruceFir, (b) high-elevation hardwoods, (c) mid-elevation hardwoods, and (d) low-elevation hardwoods. Data are shown for the three chambers per watershed in each forest type at each time. As stated in the main text, the only significant effect was for high-elevation hardwoods. Portions of these data have been published previously (Groffman et al. 2006; Groffman et al. 2009a).

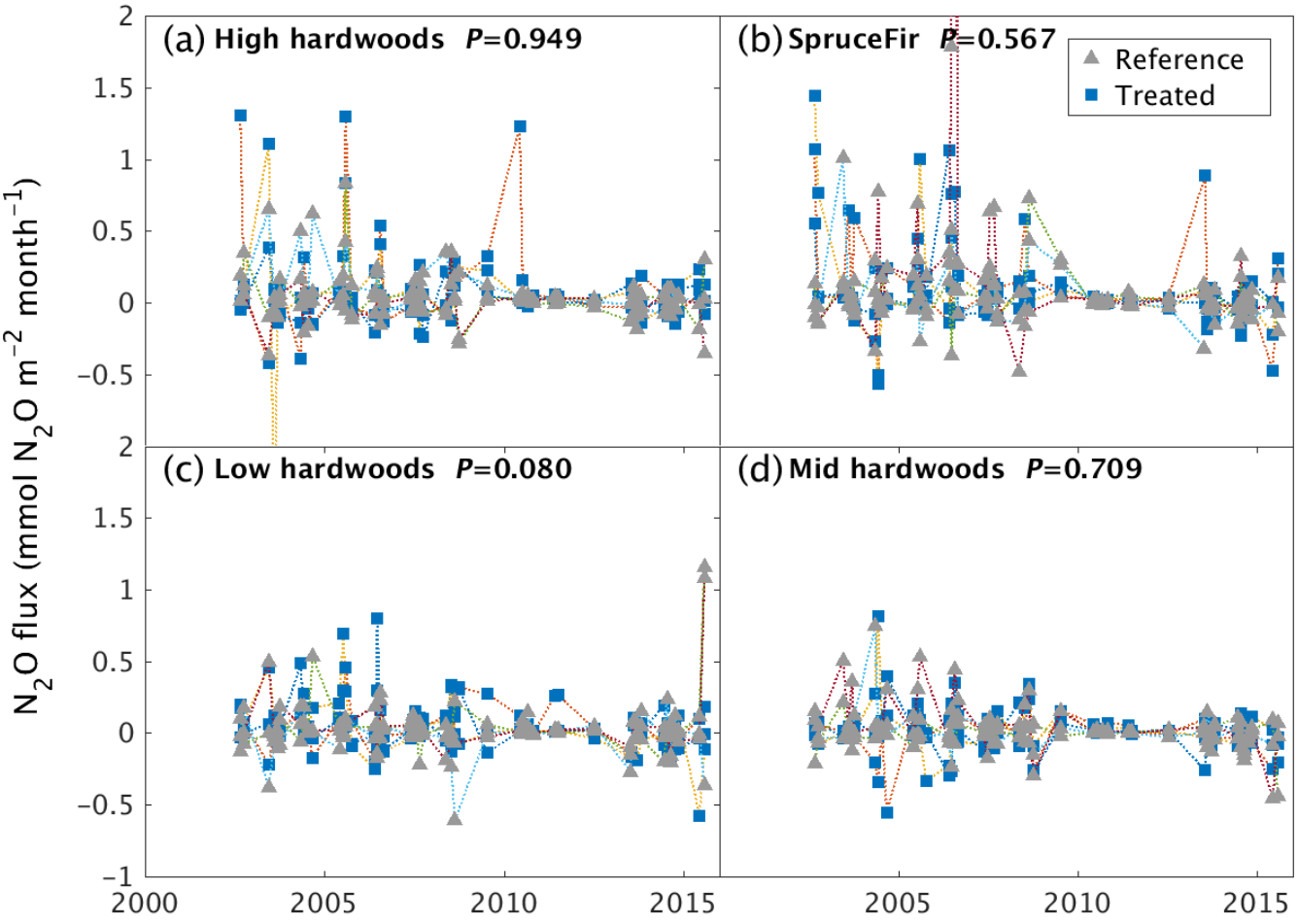

310 **Figure S8. Soil N_2O emissions for four vegetation zones:** (a) SpruceFir, (b) high-elevation hardwoods, (c) mid-elevation hardwoods, and (d) low-elevation hardwoods. Data are shown for the three chambers per watershed in each forest type at each time. Values outside the axes limits are: (a) High elevation, August 2003, chamber 3 treated watershed, -1.6502 mmol N_2O m^{-2} $month^{-1}$. (b) SpruceFir, July 2006, chamber 3 reference, 6.0540 mmol N_2O m^{-2} $month^{-1}$. As stated in the main text, there were no significant effects. Portions of these data have been published previously (Groffman et al. 2006; Groffman et al. 2018).

315

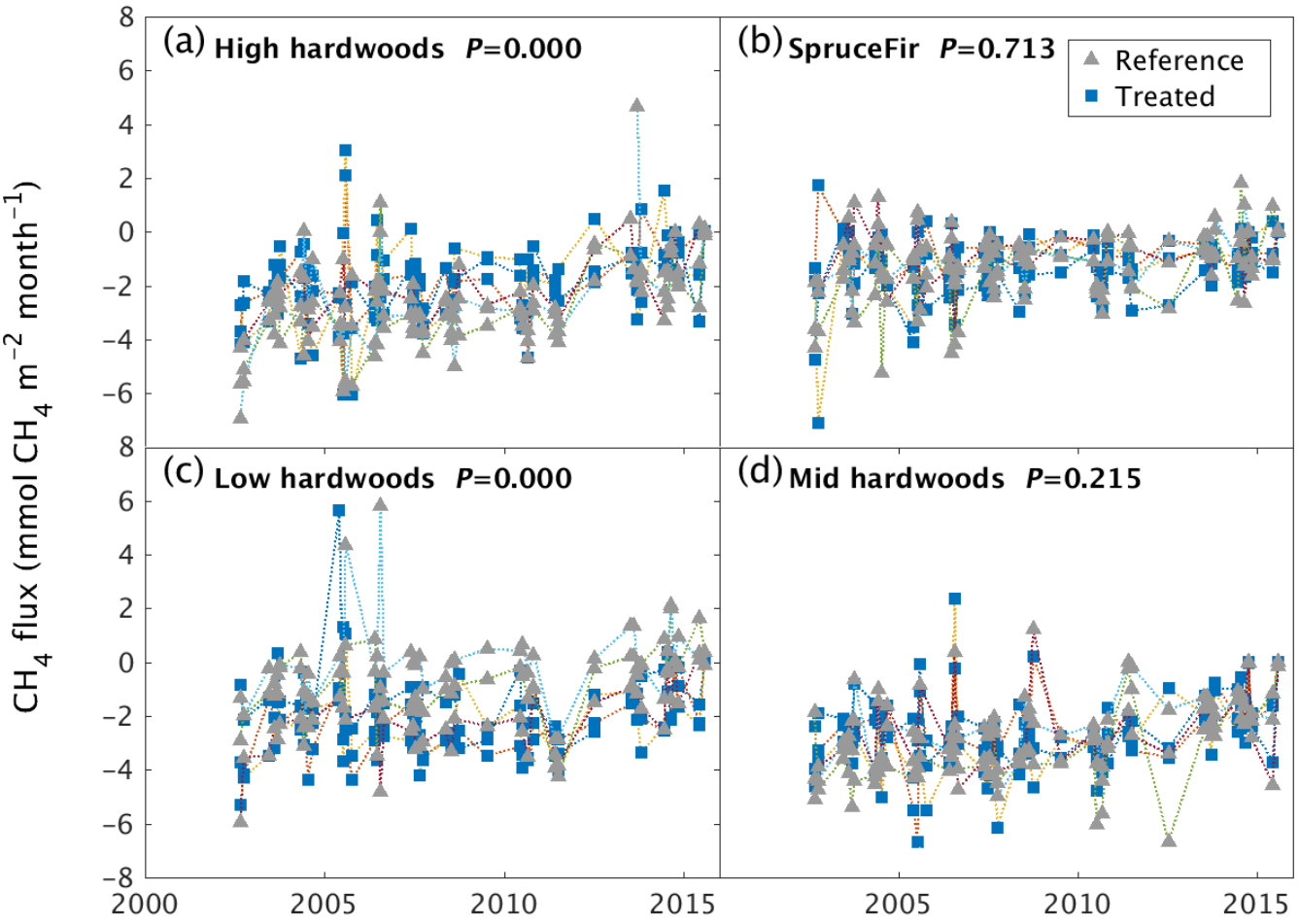

Figure S9. Soil CH_4 sink for four vegetation zones: (a) SpruceFir, (b) high-elevation hardwoods, (c) mid-elevation hardwoods, and (d) low-elevation hardwoods. Data are shown for the three chambers per watershed in each forest type at each time. As stated in the main text, the only significant effects were for low- and high-elevation hardwoods. Portions of these data have been published previously (Groffman et al. 2006; Ni and Groffman 2018).

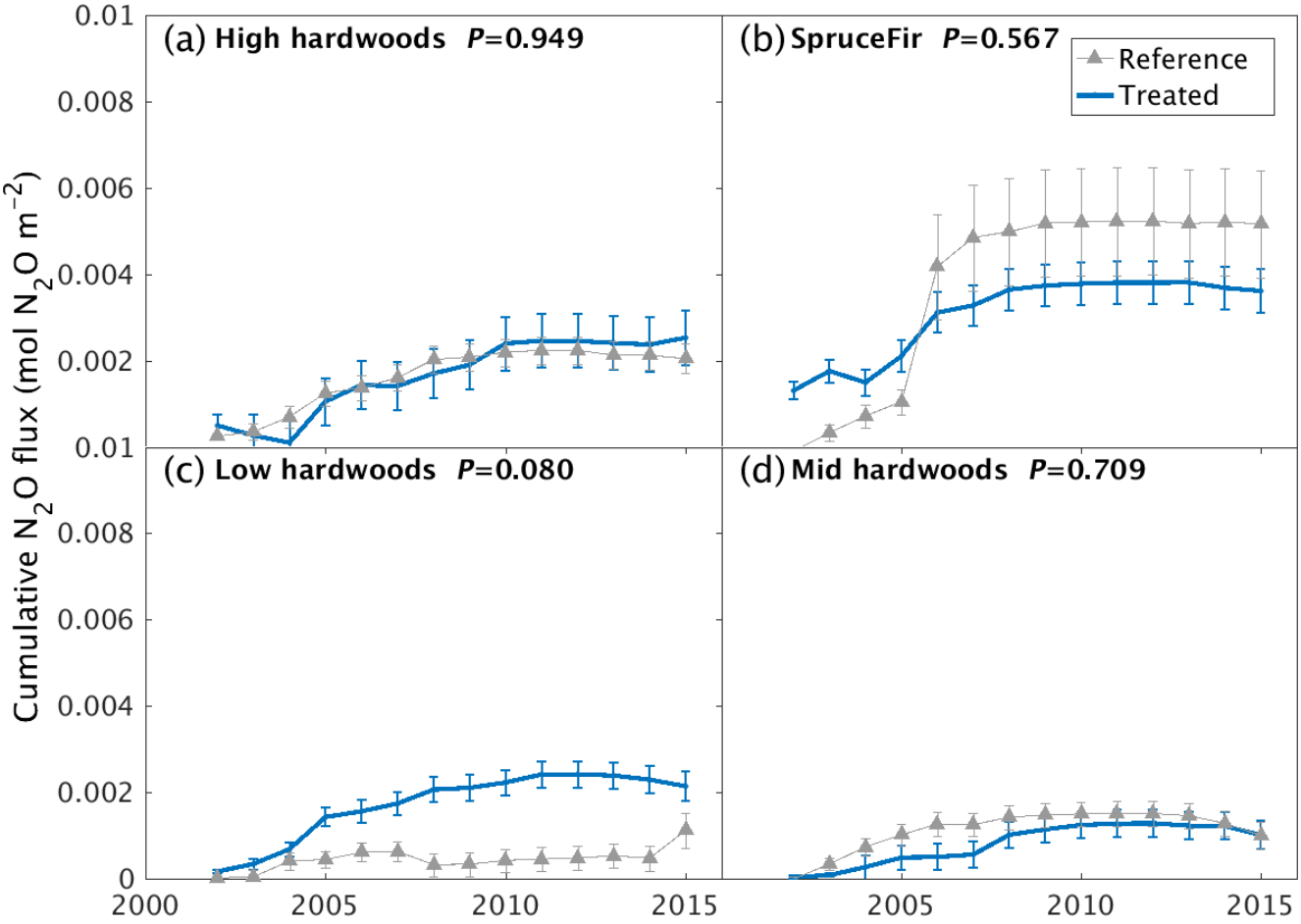

325

Figure S10. Cumulative N_2O sink for four vegetation zones: (a) SpruceFir, (b) high-elevation hardwoods, (c) mid-elevation hardwoods, and (d) low-elevation hardwoods. As stated in the main text, there were no significant effects.

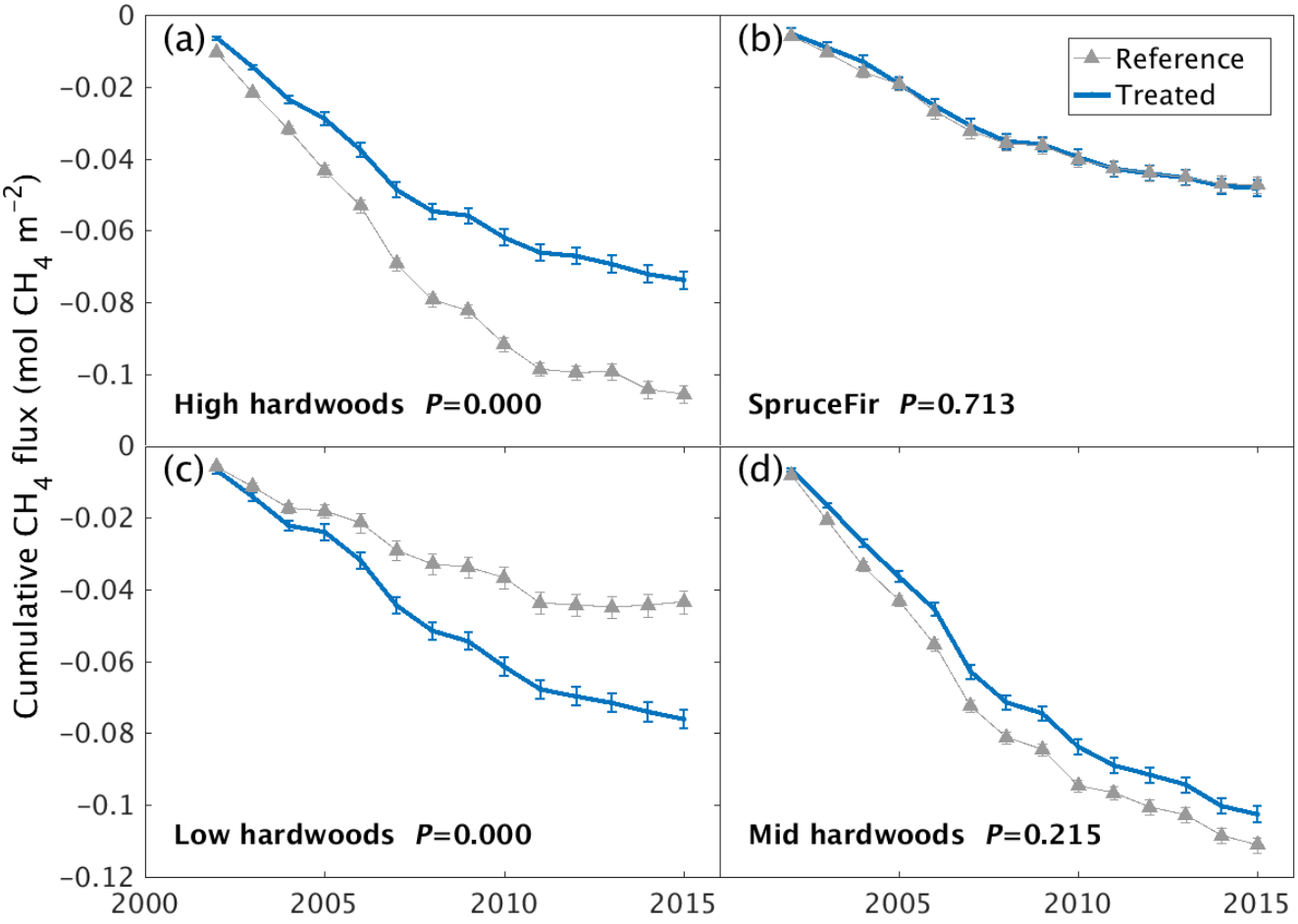

Figure S11. Cumulative CH_4 sink for four vegetation zones: (a) SpruceFir, (b) high-elevation hardwoods, (c) mid-elevation hardwoods, and (d) low-elevation hardwoods. As stated in the main text, the only significant effects were for high- and low-elevation hardwoods. Note that these effects differ: treated low-elevation hardwoods are a greater sink for CH_4 but the opposite is true for high-elevation hardwoods.

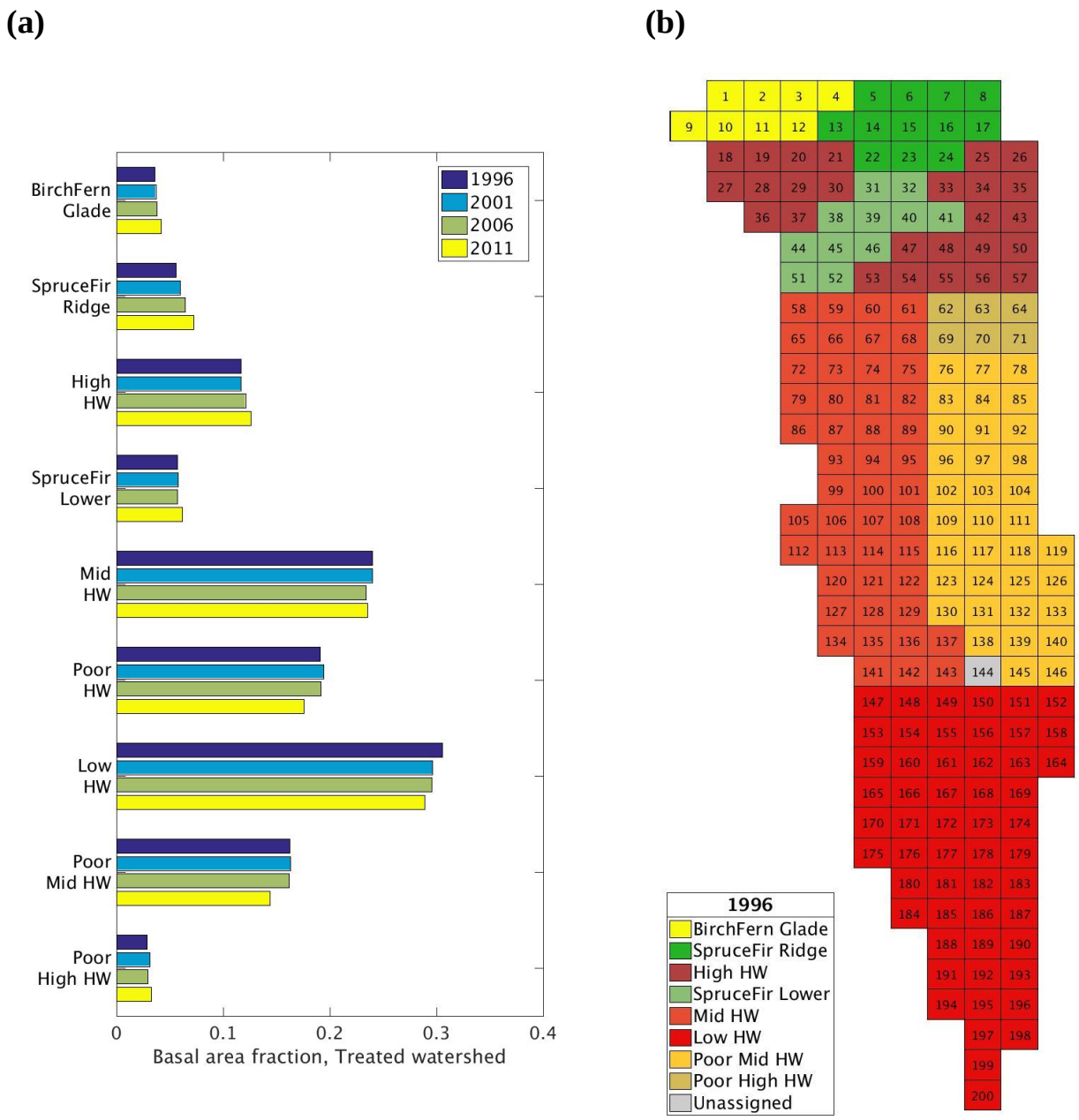

Figure S12. Basal area fraction for seven forest types in the treated watershed (Battles et al. 2015b, 2015a; Driscoll et al. 2015; Driscoll Jr et al. 2015). (a) In addition to the four forest types where we have measured greenhouse gas fluxes (SpruceFir, and Low, Mid and High elevation hardwoods), a few additional categories appear in the vegetation survey data for the treated watershed. The most widespread of these is "Poor Hardwoods", which are found to the east of the Mid and High elevation hardwoods. They were divided into "High" and "Low" elevation in the 2006 and 2011 vegetation inventories (Battles et al. 2015a, 2015b); these are depicted as Poor Mid HW and Poor High HW above and their sum = Poor HW. (b) The watershed is divided into 25x25m plots on a slope-corrected grid and we can assign these plots to the categories shown based on the elevation designations in the datafiles. Maps for 2001, 2006, and 2011 are similar, except that some plots near plot 144 have no elevation designation recorded even though they were surveyed.

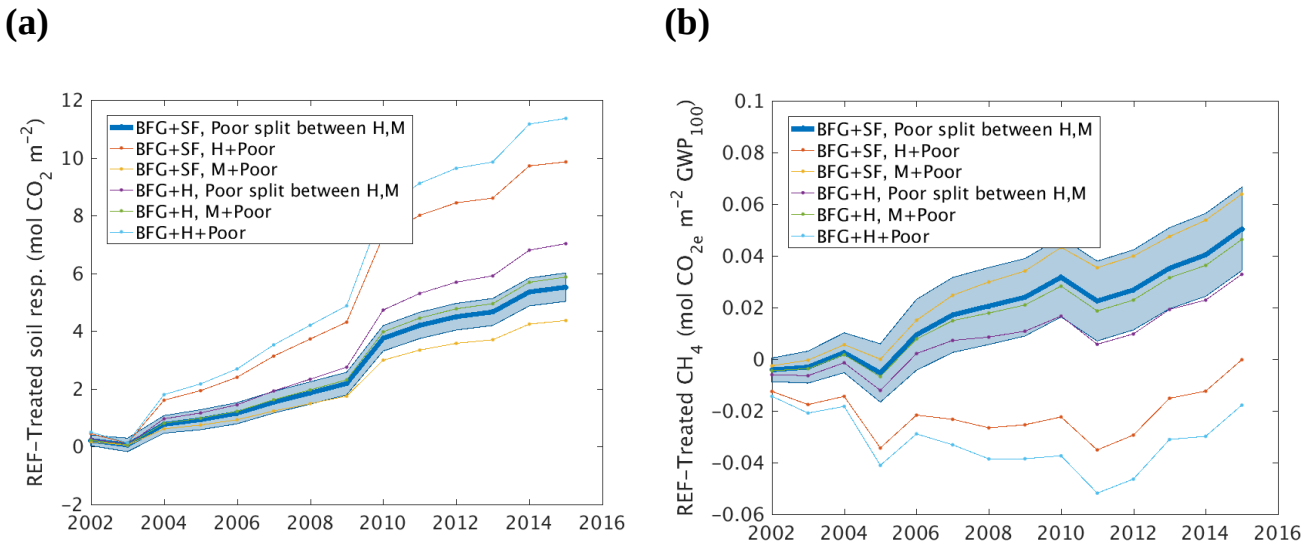

Figure S13. Mean whole-watershed greenhouse gas savings: (a) soil respiration and (b) CH_4 sink. Here we show different possibilities for combining the vegetation zones. We found no evidence for statistically significant differences in N_2O emissions. We propagated the errors using standard techniques (sum of squares of standard errors).

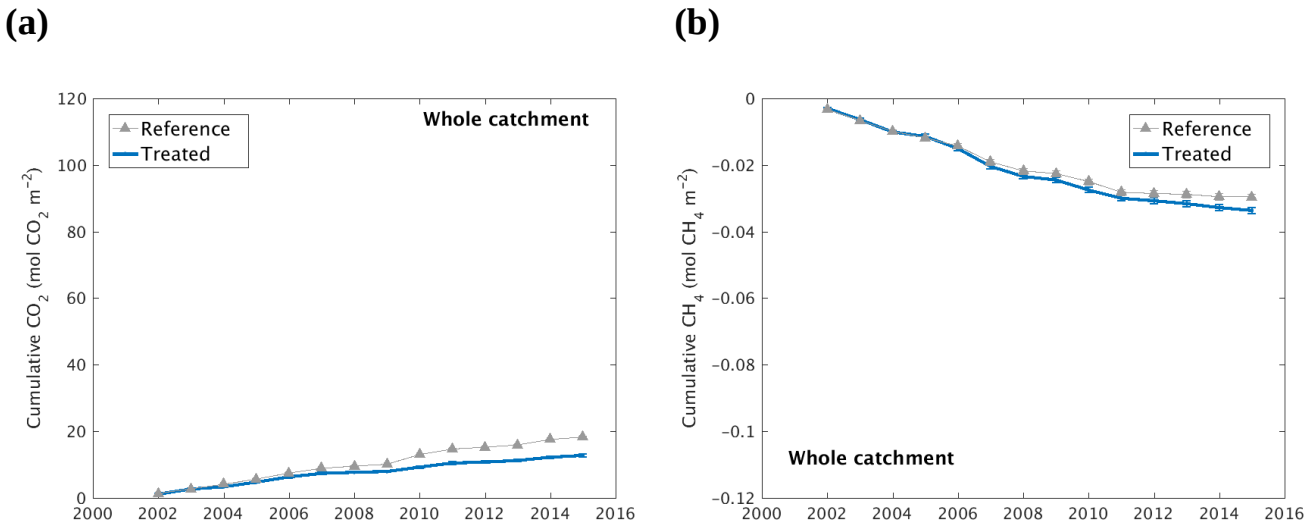

Figure S14. Whole-catchment mean cumulative (a) soil respiration and (b) soil CH_4 sink for comparison with Fig. 3 (main text) and Fig. S11. Y-axis scales match Fig. 4 and Fig. S8. In these figures, we have calculated all emissions using vegetation distributions in the treated watershed. We have not used vegetation distributions from the reference watershed for our reference curves because we were primarily interested in the probable emissions from our treated watershed, had it not been treated. The reference watershed has a different elevation range and distribution of vegetation zones. Propagated standard errors from the individual chambers are shown for each point.

360

4 Details of datasets used in this study

Here we list DOIs, filenames, package IDs and access dates of our datasets. As of the time of writing these are freely available with the exception of the latest strontium isotope data. Contact J. Blum for access to those data.

Longitudinal streamwater chemistry data, treated watershed, accessed spring 2018

365 DOI: 10.6073/pasta/fcfa498c5562ee55f6e84d7588a980d2 (Driscoll 2016a)

File: w1long_strmchem.txt Package ID: knb-lter-hbr.156.5 (*Uploaded 2016-03-01*)

Longitudinal streamwater chemistry data, reference watershed, accessed spring 2018

DOI: 10.6073/pasta/0033e820ff0e6a055382d4548dc5c90c (Driscoll 2016b)

370 File: w6long_strmchem.txt Package ID: knb-lter-hbr.127.7 (*Uploaded 2016-03-01*)

Streamwater Sr isotope and Ca/Sr, treated watershed (1997–2009, subset of our extended dataset)

DOI: 10.6073/pasta/43ebc0f959780cfc30b7ad53cc4a3d3e (Blum 2019)

File: w1_stream_isotopes.txt Package ID: knb-lter-hbr.139.3 (*Uploaded 2019-01-10*)

375 Extended data provided by J. Blum spring 2018.

Precipitation chemistry (rain/snow), treated watershed, accessed spring 2018

DOI: 10.6073/pasta/df90f97d15c28daeb7620b29e2384bb9 (Likens 2016a)

File: w1_precip_chem.txt Package ID: knb-lter-hbr.15.9 (*Uploaded 2016-02-18*)

380

Precipitation chemistry (rain/snow), reference watershed, accessed spring 2018

DOI: 10.6073/pasta/8d2d88dc718b6c5a2183cd88aae26fb1) (Likens 2016b)

File: w6_precip_chem.txt Package ID: knb-lter-hbr.20.9 (*Uploaded 2016-02-18*)

385 Daily streamflow, accessed spring 2018

DOI: 10.6073/pasta/727ee240e0b1e10c92fa28641bedb0a3 (Campbell 2015)

File: swd_all.txt Package ID: knb-lter-hbr.2.6 (*Uploaded 2016-02-01*)

Daily rain/snow precipitation, accessed spring 2018

390 DOI: 10.6073/pasta/a84c4ecb82573486e4d080d392fe64b1 (Campbell 2016a)

File: pwd_all.txt Package ID: knb-lter-hbr.14.8 (*Uploaded 2016-03-01*)

Daily mean temperature, accessed spring 2018

DOI: 10.6073/pasta/75b416d670de920c5ace92f8f3182964 (Campbell 2016b)

395 File: tdm_all.txt Package ID: knb-lter-hbr.58.7 (*Uploaded 2016-03-03*)

Soil respiration, nitrous oxide flux and methane flux, accessed summer 2018

DOI: 10.6073/pasta/9d017f1a32cba6788d968dc03632ee03 (Groffman 2016)

File: trace_gas.txt Package ID: knb-lter-hbr.116.10 (*Uploaded 2016-02-29*)

Vegetation survey data, treated watershed, 1996, accessed July 2019
DOI: 10.6073/pasta/9ff720ba22aef2b40fc5d9a7b374aa52) (Driscoll Jr et al. 2015)
File: w1_1996veg.txt Package ID: knb-lter-hbr.40.7 (*Uploaded 2019-01-09*)

Vegetation survey data, treated watershed, 2001, accessed July 2019
DOI: 10.6073/pasta/a2300121b6d594bbfcb3256ca1c300c8 (Driscoll et al. 2015)
File: w1_2001veg.txt Package ID: knb-lter-hbr.41.7 (*Uploaded 2019-01-09*)

Vegetation survey data, treated watershed, 2006, accessed July 2019
DOI: 10.6073/pasta/37c5a5868158e87db2d30c2d62a57e14 (Battles et al. 2015a)
File: w1_2006veg.txt Package ID: knb-lter-hbr.142.3 (*Uploaded 2019-01-10*)

Vegetation survey data, treated watershed, 2011, accessed July 2019
DOI: 10.6073/pasta/94f9084a3224c1e3e0ed38763f8dae02) (Battles et al. 2015b)
Filename: w1_2011veg.txt Package ID: knb-lter-hbr.143.3 (*Uploaded 2019-01-10*)

References

Arthur, MA, TG Siccama, and RD Yanai. 1999. 'Calcium and magnesium in wood of northern hardwood forest species: relations to site characteristics', *Canadian Journal of Forest Research*, 29: 339–46.

Bain, DC, and JR Bacon. 1994. 'Strontium isotopes as indicators of mineral weathering in catchments', *Catena*, 22: 201–14.

Battles, John J, Charles T Driscoll Jr, Scott W Bailey, Joel D Blum, Donald C Buso, Timothy J Fahey, Melany Fisk, Peter M Groffman, CE Johnson, and GE Likens. 2015a. 'Forest Inventory of a Calcium Amended Northern Hardwood Forest: Watershed 1, 2006, Hubbard Brook Experimental Forest. Environmental Data Initiative'.

———. 2015b. 'Forest Inventory of a Calcium Amended Northern Hardwood Forest: Watershed 1, 2011, Hubbard Brook Experimental Forest. Environmental Data Initiative'.

Battles, John J, Timothy J Fahey, Charles T Driscoll Jr, Joel D Blum, and Chris E Johnson. 2014. 'Restoring soil calcium reverses forest decline', *Environmental Science & Technology Letters*, 1: 15–19.

Bauer, James E, Wei-Jun Cai, Peter A Raymond, Thomas S Bianchi, Charles S Hopkinson, and Pierre AG Regnier. 2013. 'The changing carbon cycle of the coastal ocean', *Nature*, 504: 61–70.

Bianchi, Thomas S. 2011. 'The role of terrestrially derived organic carbon in the coastal ocean: A changing paradigm and the priming effect', *Proceedings of the National Academy of Sciences*, 108: 19473–81.

Blum, Joel D. 2019. 'Streamwater Ca, Sr and $^{87}Sr/^{86}Sr$ measurements on Watershed 1 at the Hubbard Brook Experimental Forest. Environmental Data Initiative'.

Blum, Joel D, Andrea Klaue, Carmen A Nezat, Charles T Driscoll, Chris E Johnson, Thomas G Siccama, Christopher Eagar, Timothy J Fahey, and Gene E Likens. 2002. 'Mycorrhizal weathering of apatite as an important calcium source in base-poor forest ecosystems', *Nature*, 417: 729–31.

Cai, Wei-Jun. 2011. 'Estuarine and coastal ocean carbon paradox: CO2 sinks or sites of terrestrial carbon incineration?', *Annual Review of Marine Science*, 3: 123–45.

Campbell, J. 2015. 'Hubbard Brook Experimental Forest (USDA Forest Service): Daily Streamflow by Watershed, 1956–present', *Environmental Data Initiative*.

———. 2016a. 'Hubbard Brook Experimental Forest (US Forest Service): Total Daily Precipitation by Watershed, 1956–present. Environmental Data Initiative'.

———. 2016b. 'Hubbard Brook Experimental Forest (USDA Forest Service): Daily Mean Temperature Data, 1955–present. Environmental Data Initiative'.

Canfield, Donald E, Alexander N Glazer, and Paul G Falkowski. 2010. 'The evolution and future of Earth's nitrogen cycle', *Science*, 330: 192–96.

Capo, Rosemary C, Brian W Stewart, and Oliver A Chadwick. 1998. 'Strontium isotopes as tracers of ecosystem processes: theory and methods', *Geoderma*, 82: 197–225.

Chen, Fei, Daniel G MacDonald, and Robert D Hetland. 2009. 'Lateral spreading of a near-field river plume: Observations and numerical simulations', *Journal of Geophysical Research: Oceans*, 114: C07013.

Cho, Youngil, Charles T Driscoll, Chris E Johnson, Joel D Blum, and Timothy J Fahey. 2012. 'Watershed-level responses to calcium silicate treatment in a northern hardwood forest', *Ecosystems*, 15: 416–34.

Driscoll, Charles T. 2016a. 'Longitudinal Stream Chemistry at the Hubbard Brook Experimental Forest, Watershed 1, 1991–present. Environmental Data Initiative'.

———. 2016b. 'Longitudinal Stream Chemistry at the Hubbard Brook Experimental Forest, Watershed 6, 1982–present. Environmental Data Initiative'.

Driscoll, Charles T, Scott W Bailey, Joel D Blum, Donald C Buso, Christopher Eagar, Timothy J Fahey, Melany Fisk, Peter M Groffman, CE Johnson, GE Likens, Steven P Hamburg, and Thomas G Siccama. 2015. 'Forest Inventory of a Calcium Amended Northern Hardwood Forest: Watershed 1, 2001, Hubbard Brook Experimental Forest. Environmental Data Initiative'.

Driscoll Jr, Charles T, Scott W Bailey, Joel D Blum, Donald C Buso, Christopher Eagar, Timothy J Fahey, Melany Fisk, Peter M Groffman, CE Johnson, GE Likens, Steven P Hamburg, and Thomas G Siccama. 2015. 'Forest Inventory of a Calcium Amended Northern Hardwood Forest: Watershed 1, 1996, Hubbard Brook Experimental Forest. Environmental Data Initiative'.

Duvert, Clément, David E. Butman, Anne Marx, Olivier Ribolzi, and Lindsay B. Hutley. 2018. 'CO_2 evasion along streams driven by groundwater inputs and geomorphic controls', *Nature Geoscience*, 11: 813–18.

Fahey, Timothy J, Alexis K Heinz, John J Battles, Melany C Fisk, Charles T Driscoll, Joel D Blum, and Chris E Johnson. 2016. 'Fine root biomass declined in response to restoration of soil calcium in a northern hardwood forest', *Canadian Journal of Forest Research*, 46: 738–44.

Fahey, TJ, TG Siccama, CT Driscoll, GE Likens, J Campbell, CE Johnson, JJ Battles, JD Aber, JJ Cole, and MC Fisk. 2005. 'The biogeochemistry of carbon at Hubbard Brook', *Biogeochemistry*, 75: 109–76.

Groffman, P. M., M. C. Fisk, C. T. Driscoll, G. E. Likens, T. J. Fahey, C. Eagar, and L. H. Pardo. 2006. 'Calcium additions and microbial nitrogen cycle processes in a northern hardwood forest', *Ecosystems*, 9: 1289-305.

Groffman, P.M., C.T. Discoll, J. Duran, J.L. Campbell, L. M. Christenson, T.J. Fahey, M. C. Fisk, Colin Fuss, G. E. Likens, G.M. Lovett, L. Rustad, and P. Templer. 2018. 'Nitrogen oligotrophication in northern hardwood forests', *Biogeochemistry*, 141: 123-29.

Groffman, P.M., J.P. Hardy, M. C. Fisk, J.T. Fahey, and C.T. Driscoll. 2009a. 'Climate variation and soil carbon and nitrogen cycling processes in a northern hardwood forest.', *Ecosystems*, 12: 927-43.

Groffman, Peter M, Janet P Hardy, Melany C Fisk, Timothy J Fahey, and Charles T Driscoll. 2009b. 'Climate variation and soil carbon and nitrogen cycling processes in a northern hardwood forest', *Ecosystems*, 12: 927–43.

Groffman, Peter M. . 2016. 'Forest soil: atmosphere fluxes of carbon dioxide, nitrous oxide and methane at the Hubbard Brook Experimental Forest, 1997–present. Environmental Data Initiative'.

Hartmann, Jens, and Stephan Kempe. 2008. 'What is the maximum potential for CO_2 sequestration by "stimulated" weathering on the global scale?', *Naturwissenschaften*, 95: 1159–64.

Hunt, CW, JE Salisbury, and D Vandemark. 2011. 'Contribution of non-carbonate anions to total alkalinity and overestimation of pCO 2 in New England and New Brunswick rivers', *Biogeosciences*, 8: 3069–76.

Johnson, Chris E, Charles T Driscoll, Joel D Blum, Timothy J Fahey, and John J Battles. 2014. 'Soil chemical dynamics after calcium silicate addition to a northern hardwood forest', *Soil Science Society of America Journal*, 78: 1458–68.

Likens, GE. 2016a. 'Chemistry of Bulk Precipitation at Hubbard Brook Experimental Forest, Watershed 1, 1963–present. Environmental Data Initiative'.

———. 2016b. 'Chemistry of Bulk Precipitation at Hubbard Brook Experimental Forest, Watershed 6, 1963–present. Environmental Data Initiative'.

Lovett, Gary M, Mary A Arthur, and Katherine F Crowley. 2016. 'Effects of calcium on the rate and extent of litter decomposition in a northern hardwood forest', *Ecosystems*, 19: 87–97.

Marinov, Irina, Anand Gnanadesikan, Jorge L Sarmiento, JR Toggweiler, M Follows, and BK Mignone. 2008. 'Impact of oceanic circulation on biological carbon storage in the ocean and atmospheric pCO2', *Global biogeochemical cycles*, 22: 123–45.

Minocha, Rakesh, Stephanie Long, Palaniswamy Thangavel, Subhash C Minocha, Christopher Eagar, and Charles T Driscoll. 2010. 'Elevation dependent sensitivity of northern hardwoods to Ca addition at Hubbard Brook Experimental Forest, NH, USA', *Forest Ecology and Management*, 260: 2115–24.

Nezat, Carmen A, Joel D Blum, and Charles T Driscoll. 2010. 'Patterns of Ca/Sr and $^{87}Sr/^{86}Sr$ variation before and after a whole watershed $CaSiO_3$ addition at the Hubbard Brook Experimental Forest, USA', *Geochimica et Cosmochimica Acta*, 74: 3129–42.

Ni, Xiangyin, and P.M. Groffman. 2018. 'Declines in methane uptake in forest soils', *Proceedings of the National Academy of Sciences*, www.pnas.org/cgi/doi/10.1073/pnas.1807377115.

Peters, Stephen C, Joel D Blum, Charles T Driscoll, and Gene E Likens. 2004. 'Dissolution of wollastonite during the experimental manipulation of Hubbard Brook Watershed 1', *Biogeochemistry*, 67: 309–29.

Pett-Ridge, Julie C, Louis A Derry, and Jenna K Barrows. 2009. 'Ca/Sr and 87Sr/86Sr ratios as tracers of Ca and Sr cycling in the Rio Icacos watershed, Luquillo Mountains, Puerto Rico', *Chemical Geology*, 267: 32–45.

Raymond, Peter A. 2017. 'Temperature versus hydrologic controls of chemical weathering fluxes from United States forests', *Chemical Geology*, 458: 1–13.

Renforth, Phil, and Gideon Henderson. 2017. 'Assessing ocean alkalinity for carbon sequestration', *Reviews of Geophysics*, 55: 636–74.

Rosi-Marshall, Emma J, Emily S Bernhardt, Donald C Buso, Charles T Driscoll, and Gene E Likens. 2016. 'Acid rain mitigation experiment shifts a forested watershed from a net sink to a net source of nitrogen', *Proceedings of the National Academy of Sciences*, 113: 7580–83.

Salisbury, Joseph E, Douglas Vandemark, Christopher W Hunt, Janet W Campbell, Wade R McGillis, and William H McDowell. 2008. 'Seasonal observations of surface waters in two Gulf of Maine estuary-plume systems: Relationships between watershed attributes, optical measurements and surface pCO2', *Estuarine, Coastal and Shelf Science*, 77: 245–52.

Schlesinger, William H, and Ronald Amundson. 2018. 'Managing for soil carbon sequestration: Let's get realistic', *Global Change Biology*, 00: 1–4.

Seitzinger, Sybil P, and Anne E Giblin. 1996. 'Estimating denitrification in North Atlantic continental shelf sediments.' in, *Nitrogen cycling in the North Atlantic Ocean and its watersheds* (Springer).

Shao, Shuai, Charles T Driscoll, Chris E Johnson, Timothy J Fahey, John J Battles, and Joel D Blum. 2016. 'Long-term responses in soil solution and stream-water chemistry at Hubbard Brook after experimental addition of wollastonite', *Environ. Chem*, 13: 528–40.

Stumm, W, and J Morgan. 1996. *Aquatic Chemistry: Chemical Equilibria and Rates in Natural Waters*.

Virta, Robert L. 2000. 'Minerals Yearbook: Wollastonite', Unites States Geological Survey National Minerals Information Center, Accessed 11 September https://www.usgs.gov/centers/nmic/wollastonite-statistics-and-information.

Williamson, Phillip, Douglas WR Wallace, Cliff S Law, Philip W Boyd, Yves Collos, Peter Croot, Ken Denman, Ulf Riebesell, Shigenobu Takeda, and Chris Vivian. 2012. 'Ocean fertilization for geoengineering: a review of effectiveness, environmental impacts and emerging governance', *Process Safety and Environmental Protection*, 90: 475–88.